THE JOURNAL OF BIOLOGICAL CHEMISTRY VOL. 281, NO. 12, pp. 7952–7959, March 24, 2006

Leishmania major Expresses a Single Dihydroxyacetone Phosphate Acyltransferase Localized in the Glycosome, Important for Rapid Growth and Survival at High Cell Density and Essential for Virulence*

Received for publication, December 2, 2005, and in revised form, January 17, 2006 Published, JBC Papers in Press, January 19, 2006, DOI 10.1074/jbc.M512911200

Rachel Zufferey[1] **and Choukri Ben Mamoun**[2]

From the Department of Genetics and Developmental Biology and the Department of Molecular, Microbial and Structural Biology, University of Connecticut Health Center, Farmington, Connecticut 06030-3301

Despite major advances in the understanding of pathogenesis of the human protozoan parasite *Leishmania major*, little is known about the enzymes and the primary precursors involved in the initial steps of synthesis of its major glycerolipids including those involved in virulence. We have previously demonstrated that the initial step of acylation of the precursor glycerol 3-phosphate is not essential for the synthesis of ester and ether phospholipids in this parasite. Here we show that *Leishmania* expresses a single acyltransferase with high specificity for the precursor dihydroxyacetone phosphate and shows the best activity in the presence of palmitoyl-CoA. We have identified and characterized the *LmDAT* gene encoding this activity. *Lm*DAT complements the lethality resulting from the loss of both dihydroxyacetone phosphate and glycerol-3-phosphate acyltransferase activities in yeast. Recombinant *Lm*DAT exhibits biochemical properties similar to those of the native enzyme of the promastigote stage parasites. We show that *Lm*DAT is a glycosomal enzyme and its loss in a Δ*lmdat*/Δ*lmdat* null mutant results in complete abrogation of the parasite dihydroxyacetone phosphate acyltransferase activity. Furthermore, lack of *Lm*DAT causes a major alteration in parasite division during the logarithmic phase of growth, an accelerated cell death during stationary phase, and loss of virulence. Together, our results demonstrate that *Lm*DAT is the only dihydroxyacetone phosphate acyltransferase of the *L. major* localized in the peroxisome, important for growth and survival and essential for virulence.

Worldwide, protozoan parasites of the genus *Leishmania* cause a large spectrum of important human diseases collectively named leishmaniasis. These parasites develop within the digestive tract of the sand fly vector as flagellated, mobile promastigotes and differentiate into and multiply as non-motile amastigotes within the phagolysosomal compartment of vertebrate host macrophages.

Glycerolipids constitute 70% of total lipids in the protozoan parasite *Leishmania* (1–3). They are classified into ester and ether lipids depending on the substitution at position 1 of the glycerol backbone. Ester lipids harbor an acyl group, whereas ether lipids carry a fatty alcohol moiety. Lipids of *Leishmania* parasites have been a focus of extensive studies because some of their derivatives, such as lipophosphoglycan and glycosylphosphatidylinositol-anchored protease gp63, were shown to be important for parasite virulence and development (for review, see Refs. 4–8). Lipids are also essential cell constituents and, therefore, must be constantly synthesized to allow multiplication of the parasite. This suggests that the pathways leading to their synthesis are essential for parasite proliferation and pathogenesis and, thus, offer a reasonable target for rational design of new anti-leishmanial drugs. In fact, a lipid-based drug, miltefosine, is a potent antileishmanial compound that inhibits parasite growth *in vitro* and *in vivo* and is currently used for treatment of visceral and mucocutaneous forms of leishmaniasis (9–12). The acylation of dihydroxyacetone phosphate (DHAP)[3] by a DHAP acyltransferase (DHAPAT) represents the initial and obligatory step in the biosynthesis of ether lipids in most organisms that synthesize alkylglycerolipids (13). The product of this first acylation reaction, 1-acyl-DHAP, is then converted to 1-alkyl-DHAP by a FAD-dependent alkyl DHAP synthase (14), which is further reduced to 1-alkyl-glycerol-3-phosphate (1-alkyl-G3P) by an NADPH-dependent 1-alkyl/acyl-DHAP reductase. 1-Alkyl-G3P serves as the obligate precursor for all ether phospholipids. Alternatively, 1-acyl-DHAP can be reduced to 1-acyl-G3P by an NADPH-dependent 1-alkyl/1-acyl-DHAP reductase, which is then used for the biosynthesis of ester phospholipids. The relative contribution of the DHAP acylation step in the biosynthesis of ester phospholipids has not yet been firmly established (15, 16).

DHAPAT activity has been characterized biochemically in different organisms (17–19). In most animal tissues, DHAPAT is found in a membrane-bound fraction (15, 20) and localized in the luminal side of peroxisomes (15, 21). This enzyme was also found to be part of a heterotrimeric complex that includes the 1-alkyl-DHAP synthase (22, 23). Alterations in DHAPAT function have been associated with various human diseases such as neonatal adrenoleukodystrophy, infantile Refsum, disease, hyperpipecolic academia, and rhizomelic chondrodyplasia punctata (24–26).

We have previously reported the characterization of the first acyltransferase *Lm*GAT specific for the lipid precursor G3P. We showed that this activity was encoded by a single gene, *LmGAT*, whose deletion resulted in a major defect in the synthesis of triacylglycerols but had little or no effect on the biosynthesis of ester and ether phospholipids, suggesting that G3P is not the primary lipid precursor for membrane biogenesis in *Leishmania* promastigotes (27). In an attempt to evaluate the importance of dihydroxyacetone phosphate in parasite lipid metab-

* This project was supported by grants from the National Institutes of Health and Department of Defense (to C. B. M.). The costs of publication of this article were defrayed in part by the payment of page charges. This article must therefore be hereby marked "*advertisement*" in accordance with 18 U.S.C. Section 1734 solely to indicate this fact.

[1] Present address: Dept. of Biochemistry, Kansas State University, 104 Willard Hall, Manhattan, KS 66506.

[2] To whom correspondence should be addressed: Dept. of Genetics and Developmental Biology, University of Connecticut Health Center, 263 Farmington Ave, Farmington, CT 06030-3301. Tel.: 860-679-3544; Fax: 860-679-8345; E-mail: Choukri@up.uchc.edu.

[3] The abbreviations used are: DHAP, dihydroxyacetone phosphate; DHAPAT, DHAP acyltransferase; G3P, glycerol 3-phosphate; GPAT, glycerol-3-phosphate acyltransferase; PrI, propidium iodide; CHAPS, 3-[(3-cholamidopropyl)dimethylammonio]-1-propanesulfonic acid; PrI, propidium iodide.

TABLE 1
Yeast strains used in this work

Strains	Genotype	Source
cmy228 (Sc21)	MATa his3-11,15 leu2-3,112 trp1-1 ade2-1 can1-100 gat1Δ::*TRP1 gat2Δ::HIS3 ura3-1* [*pGAL1::GAT1 URA3*]	Ref. 32
gat1Δgat2Δ+[*GAL1::GAT1*]+[*ADH1::LmDAT*] (Sc9)	*MATa his3-11,15 leu2-3,112 trp1-1 ade2-1 can1-100 gat1Δ::TRP1 gat2Δ::HIS3 ura3-1* [*pGAL1::GAT1 URA3*] [*pBEVY-L.LmDAT*]	This work
gat1Δgat2Δ+[*GAL1::GAT1*]+[*ADH1*] (Sc4)	*MATα his3-11,15 leu2-3,112 trp1-1 ade2-1 can1-100 gat1Δ::TRP1 gat2Δ::HIS3 ura3-1* [*pGAL1::GAT1 URA3*] [*pBEVY-L*]	This work
gat1Δgat2Δ+[*ADH1::LmDAT*] (Sc12)	*MATa his3-11,15 leu2-3,112 trp1-1 ade2-1 can1-100 gat1Δ::TRP1 gat2Δ::HIS3 ura3-1* [*pBEVY-L.LmDAT*]	This work

olism and development, we have isolated and characterized the gene *LmDAT* encoding the DHAPAT enzyme involved in the acylation of this precursor. We provide evidence that *Lm*DAT is the only dihydroxyacetone phosphate acyltransferase of the parasite, residing in peroxisome-like organelles termed glycosomes in *Leishmania* and related parasites, important for optimal growth during the exponential phase and for survival at high cell density and essential for virulence. These data suggest that acylation of DHAP may represent the major pathway for the synthesis of glycerolipids in *Leishmania*.

EXPERIMENTAL PROCEDURES

Strains and Growth Conditions—Promastigotes of *Leishmania major* Friedlin V1 strain (MHOM/IL/80/Friedlin) were maintained in liquid and semi-solid M199-derived medium (28). Transfection was performed according to Ngo *et al.* (29), and selection was applied as appropriate in the presence of G418, nourseothricin, blasticidin, or puromycin (10, 150, 5, and 50 μg/ml, respectively). To examine parasite proliferation, parasites were collected at mid-log phase, diluted to 5×10^5 parasites/ml, and incubated at 26 °C. Growth was monitored by collecting samples over time and counting them using a hemacytometer. Limiting dilution assays were carried out by diluting parasite cultures with fresh media to 5 parasites/ml. 200-μl samples of this diluted culture were transferred into a 96-well plate. The plates were incubated for 2 weeks at 26 °C, and the presence of parasites was monitored by light microscopy.

Saccharomyces cerevisiae strains used in this study are listed in Table 1. Yeast was cultivated at 30 °C in YPD (1% Bacto-yeast extract, 2% Bacto-peptone, and 2% glucose), YPGal (1% Bacto-yeast extract, 2% Bacto-peptone, and 2% galactose), or synthetic minimal media supplemented as required to maintain cell growth. Limiting dilutions on solid YPD and YPGal plates were performed as described previously (27).

Plasmids—LmDAT was PCR-amplified from *L. major* genomic DNA using the primer pair BN-LmDHAPAT-5′ (′5-CGGGATCCCATATGAGCTTCCCACCACCTCGG-3′) and LmDHAPAT-B-3′ (′5-CGGGATCCTCACATCTTGGATGGCTGTGTT-3′). The resulting PCR product was digested with BamHI and ligated to the BamHI site of pUC19 (New England Biolabs) in sense orientation to yield pUC19.LmDAT (Ec207). pBEVY-L.LmDAT (Ec210) was obtained by subcloning the 4.3-kilobase BamHI (partial)-XbaI fragment of pUC19.LmDAT into the BamHI and XbaI sites of pBEVY-L (30). The plasmid pL-BSD (Ec221) was constructed as follows; the *BSD* cassette was PCR-amplified with the primers 5-XbaI-BSD (5′-GCTCTAGATGCCTTTGTCTCAAGAAGAATC-3′) and 3-XbaI-BSD (5′-GCTCTAGATTAGCCCTCCCACACATAAC-3′) and pTEF1/BSD (Invitrogen) as template, digested with XbaI, and ligated into the SpeI sites of pXG.SAT (28) in sense orientation. To obtain the pL-BSD.HV-LmDAT (Ec247) plasmid, pL-BSD.LmDAT (Ec237) was first constructed by subcloning the 4.3 kilobases BamHI fragment of pUC19.LmDAT into the BamHI site of pL-BSD with the transcription orientation of the *LmDAT* gene similar to the *BSD* marker. Then a PCR reaction using the oligonucleotides B-His_6-V5-LmDAT (5′-CGGGATCCATGCATCATCACCATCACCATGGTAAGCCTATCCCTAACCCTCTCCTCGGTCTCGATTCTACGATGAGCTTC-CCACCACCTC-3′) and LmDHAPAT-424r (5′-AGTTCGTCTCGCCAAGTG-3′) and pUC19.LmDAT as a template was performed, and the resulting PCR product was digested with BamHI and EcoRI. The resulting 0.4-kilobase fragment was used to replace the corresponding non-tagged coding DNA region of pL-BSD.LmDAT digested with BamHI and EcoRI.

To delete the chromosomal *LmDAT* gene, the following plasmids were generated. First, the 5′-untranslated region of *LmDAT* was amplified with LmDAT-1778-B (′5-GGGGATCCAATGCATGTGTGC-3′) and LmDAT-752-E (′5-CAGAATTCGAAGAGGGAGCTAAAGG-3′). The resulting PCR products were digested with BamHI and EcoRI and cloned into the corresponding sites of pBluescript II KS (+/−) (Stratagene), yielding pBS-5′U-LmDAT (Ec216). The 3′-untranslated region of *LmDAT* was amplified with LmDAT+1-S (′5-GAGGAGCTCGTGTAGACCTGTGTC-3′) and LmDAT+801-K (′5-CGAGGTACCGCGAAGACATCAATATTG-3′) followed by TA cloning into pCR2.1 (Invitrogen), resulting in pCR-3′U-LmDAT (Ec219). The 3′-untranslated region was excised from pCR-3′U-LmDAT after digestion with EcoRI and KpnI and ligated to the EcoRI and KpnI sites of pBS-5′U-LmDAT to give pBS.5′3′U-LmDAT (Ec220). The nourseothricin (*SAT*) and puromycin (*PAC*) cassettes were isolated from pXG.SAT (28) and pX63PAC (31), respectively, by digestion with EcoRI and SacI and ligated to the EcoRI and SacI sites of pBS.5′3′U-LmDAT yielding pBS.LmDAT:SAT (Ec231) and pBS.LmDAT:PAC (Ec225), respectively. All PCR-generated products were verified by sequencing.

Yeast Complementation—Cmy228 (*gat1Δgat2Δ*+[*pGAL1::GAT1 URA3*] (32)) was transformed with pBEVY-L.LmDAT, yielding cmy228+[*ADH1::LmDAT*] (*gat1Δgat2Δ*+[*pGAL1::GAT1 URA3*]+[*pBEVY-L.LmDAT*]). Contra-selection to discard the (*pGAL1::GAT1 URA3*) episome was achieved in the presence of 5-fluoroorotate, yielding *gat1Δgat2Δ*+[*ADH1::LmDAT*]. The presence of *GAT1* was verified by PCR using the oligonucleotides ScSCT2–749 (′5-ATACGAAGGGCTGTGTAGG-3′) and ScSCT2–1697 (′5-TCAACACCGATTTCACCG-3′). The presence of *LmDAT* was verified using the primer pair LmDAT-3531 (′5-GTTCGGCTTCGTCACAAC-3′) and LmDHAPAT-B-3′ (′5-CGGGATCCTCACATCTTGGATGGCTGTGTT-3′). The *HNM1* gene was PCR-amplified using the primer pair OCHO47 (′5-CATTGCTTGTCACACTTGG-3′) and OCHO78 (′5-CCGCTCGAGCTGCAGTCACTTCTTTCCCCACGGTAC-3′).

Activity Assays—The yeast strain *gat1Δgat2Δ*+[*ADH1::LmDAT*] was grown in YPD to an A_{600} of 0.8–1.0. Cells were washed twice in ice-cold water, and cell pellets were frozen at −80 °C until use. Yeast and *Leishmania* protein extracts were prepared as described previously (27, 33). Protein concentration was determined by the bicinchoninic acid assay using bovine serum albumin as a standard. Glycerol-3-phosphate acyltransferase (GPAT) activity was measured as previously described (27) using 100–200 μg of protein. DHAPAT activity was

assessed by measuring the acylation rate of DHAP. This substrate was synthesized from fructose-1,6-bisphosphate as described by Bates and Saggerson (34). The assay was performed in a 0.5-ml final volume in a buffer containing 120 mM KCl, 50 mM Tris-HCl (pH 7.5), 4 mM $MgCl_2$, 8 mM NaF, 4 mg/ml fatty acid poor albumin, 100 μM acyl-CoA, 0.25 unit of aldolase, 7 units of triose phosphate isomerase, 0.1% CHAPS, and 0.5–1 mg of protein. Assays were performed at 30 °C unless otherwise stated. For the pH-dependent DHAPAT assay, a 100 mM sodium phosphate buffer set up at different pH values was used. The specificity of L-[U-^{14}C]glycerol 3-phosphate (Amersham Biosciences) and D-[*fructose*-U-^{14}C] 1,6-bisphosphate (MP Biomedicals) were 149 and 295 mCi/mmol, respectively. DHAPAT and GPAT reaction products were verified by analytical thin layer chromatography using Silica Gel 60A plates (Whatman) and a solvent made of chloroform, methanol, acetic acid, 5% aqueous sodium metabisulfite (75:30:9:3, v/v/v/v). The plates were sprayed with EN^{3}HANCE (PerkinElmer Life Sciences) before autoradiography. The R_f values for 1-acyl-G3P and 1-acyl-DHAP were 2.1 and 3.5, respectively.

Malate dehydrogenase assay was performed in 0.1 M potassium phosphate buffer, pH 7.4, containing 0.21 mM oxaloacetate and 0.26 mM NADH. The assay was initiated by the addition of 20 μg of *Leishmania* protein extracts, and the decrease in absorbance was monitored spectrophotometrically at a wavelength of 340 nm.

Microscopy—Differential interference contrast (DIC) analysis was performed using promastigotes fixed with 4% paraformaldehyde in phosphate-buffered saline and mounted on polylysine-coated slides. Immunofluorescence assay was performed with wild-type parasites alone or transformed with pL-BSD.HV-LmDAT (Ec247) as described previously (28). The recombinant His_6-V5 tagged HV-*Lm*DAT was revealed with V5 monoclonal antibodies (Invitrogen) and hypoxanthine-guanine phosphoribosyltransferase with specific rabbit polyclonal immunoglobulins (generous gifts of A. Jardim). Both antibodies were used at a 1:500 dilution. Images were taken with a Nikon fluorescence microscope.

Analysis of Cell Death—Parasites were washed once in phosphate-buffered saline and stained in the presence of 1 μg/ml propidium iodide (PrI) in phosphate-buffered saline for 10 min before being analyzed by flow cytometry.

Virulence Assays in Mice—Virulence assays were performed as described in Zufferey *et al.* (28). Briefly, parasites derived from a 3-day stationary culture were washed once in cold saline buffer. 1×10^6 or 1×10^7 cells were injected subcutaneously in the right rear footpad of 6–8-week-old female BALB/c mice (Charles River Laboratory). Infections were monitored by comparing the thickness of the footpad over time using a Vernier caliper.

RESULTS

Characterization of the Dihydroxyacetone Phosphate Acyltransferase Activity in L. major Promastigotes—Our genetic and biochemical characterization of the *L. major* GPAT enzyme *Lm*GAT suggested that the lipid precursor G3P does not play an essential function in parasite development or biosynthesis of its major acyl- and alkylglycerolipids. To examine the importance of the second lipid precursor DHAP in parasite membrane biogenesis and development, we characterized its first acylation step (DHAPAT activity) in whole cell extracts. DHAPAT activity was linear during ~8 min of incubation and reached a plateau thereafter when measured at 30 °C (Fig. 1*A*). When the assay was performed at 0 °C, only marginal activity could be detected, indicating that this reaction is enzymatic. Kinetic studies were conducted by varying the concentration of fructose 1,6-bisphosphate to obtain a substrate saturation curve. DHAPAT activity reached its maximum when the substrate concentration was ~2 mM (Fig. 1*B*). From these data, a V_{max} of 208.8 ± 33.6 pmol/min × mg and a K_m of 0.47 ± 0.1 mM could be calculated, indicating that DHAPAT activity in *Leishmania* involves a relatively low affinity DHAPAT enzyme(s). The specificity of DHAPAT was assessed by testing different fatty acyl-CoA donors that differ in length and/or saturation. The best activities were obtained when palmitoyl-CoA was present in the assay, whereas myristoyl-CoA, stearoyl-CoA, and linoleoyl-CoA all resulted in lower activities. The least effective fatty acyl-CoA donors were dodecyl-, palmitoleoyl-, oleoyl-, and arachidoyl-CoA (Fig. 1*C*).

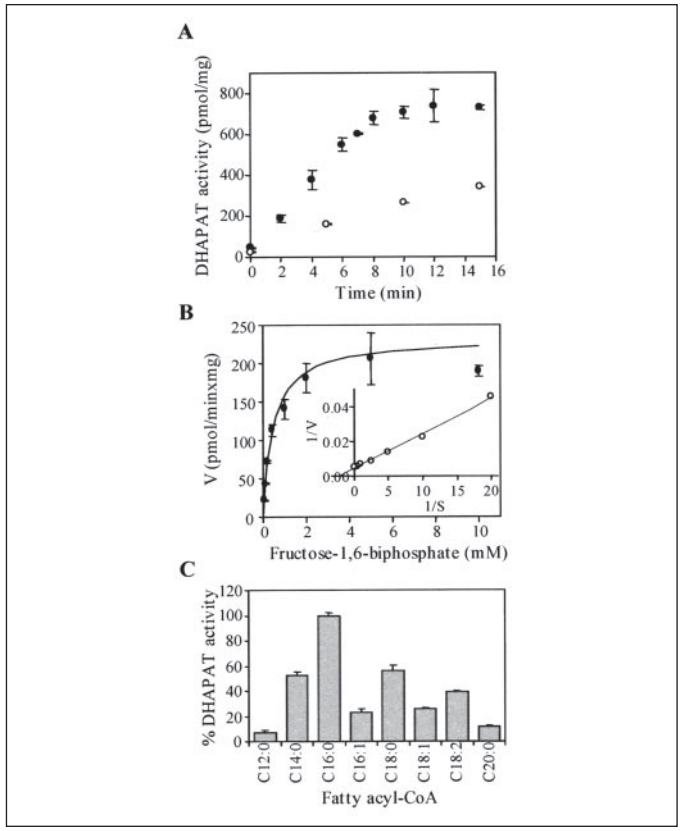

FIGURE 1. **DHAPAT activity in *L. major* promastigotes.** The acylation rate of DHAP produced by catabolism of fructose 1,6-bisphosphate by an aldolase and triose phosphate isomerase was measured as described under "Experimental Procedures." *A*, time-dependent acylation of DHAP in *Leishmania* whole cell extracts carried out at 0 or 30 °C (*open* and *closed circles*, respectively) in the presence of 100 μM stearoyl-CoA and 1 mg of protein as described under "Experimental Procedures". *B*, kinetics of DHAPAT activity in *Leishmania* protein extracts. Substrate saturation curve was fitted to the Michaelis-Menten equation, $V = V_{max} \times S/(K_m + S)$. The Lineweaver-Burk double reciprocal plot is shown in the inset. K_m and V_{max} were calculated to be 0.47 ± 0.1 mM and 208.8 ± 33.6 pmol/min × mg. *C*, substrate specificity of DHAPAT activity. The reactions were incubated for 5 min at 30 °C in the presence of 100 μM fatty acyl-CoA. All assays were performed at least twice in duplicate, and only one representative experiment is shown here. S.D. are depicted.

Identification of LmDAT—To isolate the gene encoding the *L. major* DHAPAT activity, we searched the *L. major* genome for proteins harboring the four signature motifs important for acyltransferase activity (35). In addition to the *LmGAT* gene, we identified an open reading frame of ~4.3 kilobases encoding a protein of 1436 amino acids, which we termed *Lm*DAT (for dihydroxyacetone phosphate acyltranferase) that exhibits significant similarity (~35% identity and ~55% similarity) to other eukaryotic DHAPATs (Fig. 2*B*). The most conserved region in the enzyme encompasses amino acids 680–975 and harbors the four canonical domains involved in substrate recognition and catalysis (Fig. 2*B* (35, 36)). Interestingly, unlike human and other higher eukaryotic

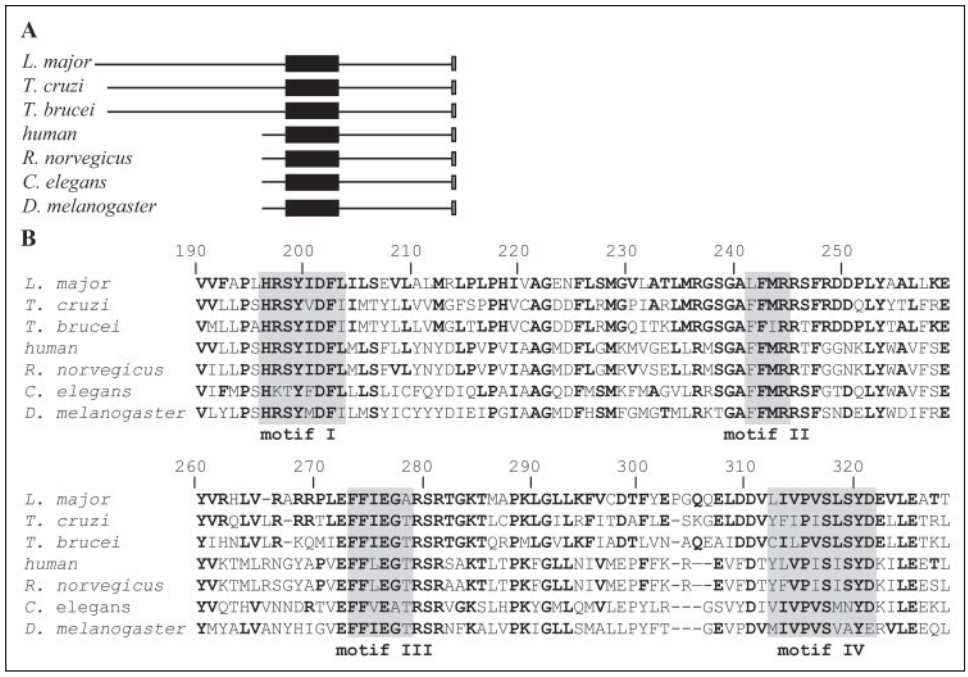

FIGURE 2. **DHAPAT sequence alignment.** *A*, schematic representation of DHAPAT orthologs from *T. cruzi*, *T. brucei*, human, rat (*Rattus norvegicus*), *Caenorhabditis elegans*, and fruit fly (*Drosophila melanogaster*). The domain containing the four conserved blocks diagnostic of G3P and DHAP acyltransferases are depicted as *black rectangles*. The C-terminal glycosomal/peroxisomal tripeptide is represented by an *open rectangle*. *B*, sequence alignment of the catalytic/substrate recognition domain of DHAPATs of *L. major*, *T. cruzi*, *T. brucei*, human, rat, *C. elegans*, and *D. melanogaster*. *Numbers* correspond to the amino acid position of *L. major Lm*DAT protein sequence. Amino acids identical to *Lm*DAT are in *bold*, and *shaded motifs* represent the four GPAT/DHAPAT diagnostic blocks.

DHAPATs, *Lm*DAT contains an unusual N-terminal domain of ~650 amino acids. Homologs of *Lm*DAT in the Trypanosomatidae family such as *Trypanosoma cruzi* and *Trypanosoma brucei* also harbor this N-terminal domain and share a high degree of identity and similarity with *Lm*DAT over the whole protein length. A specific homology search of available protein databases with this N-terminal domain failed to identify any similarity to known proteins. The C-terminal domain of *Lm*DAT contains a signature tripeptide SKM for localization to the glycosomes (37).

Subcellular Localization of LmDAT—To determine the cellular localization of *Lm*DAT, a hexahistidine-V5 tag was added to the N-terminal portion of the enzyme, and the resulting recombinant protein (HV-*Lm*DAT) was expressed in wild-type *Leishmania*. Immunofluorescence analysis using a V5-specific monoclonal antibody revealed a signal diagnostic of glycosomal proteins. Indeed colocalization studies revealed a perfect colocalization between HV-*Lm*DAT and the glycosomal marker, hypoxanthine-guanine phosphoribosyltransferase (38) (Fig. 3). No signal could be detected in non-transfected cells using anti-V5 antibody (Fig. 3). These data suggest that *Lm*DAT is localized to the glycosomes (21).

Functional Analysis of LmDAT in Yeast—We have previously shown that the yeast *S. cerevisiae* can be used as a surrogate system to genetically and biochemically analyze the function of heterologous GPAT enzymes (27, 33). Yeast harbors two acyltransferases, GAT1 and GAT2, which catalyze the acylation of both G3P and DHAP (32, 39). *GAT1*$^{+}$*gat2*Δ and *gat1*Δ*GAT2*$^{+}$ single deletion mutants are viable, whereas a double mutant, *gat1*Δ*gat2*Δ, is lethal. To genetically assess the function of *LmDAT*, we examined whether *LmDAT* can rescue the lethal phenotype of the yeast double mutant *gat1*Δ*gat2*Δ lacking the *GAT1* and *GAT2* genes (32, 39). To this end, we generated a strain *gat1*Δ*gat2*Δ+[*GAL1*::*GAT1*]+[*ADH1*::*LmDAT*] that expresses *LmDAT* under the constitutive *ADH1* promotor in the strain cmy228 (*gat1*Δ*gat2*Δ+[*pGAL1*::*GAT1 URA3*] (32)). This strain bears chromosomal deletions of *GAT1* and *GAT2* but expresses episomally the endogenous *GAT1* under the control of the inducible *GAL1* promotor. A control strain, *gat1*Δ*gat2*Δ+[*GAL1*::*GAT1*]+[*ADH1*], which carries the vector alone, was also generated. Both strains were serially diluted

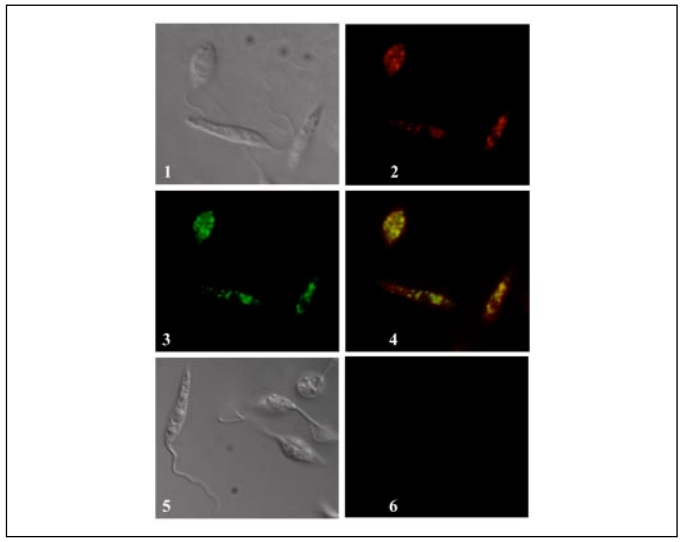

FIGURE 3. ***Lm*DAT is localized to the glycosomes.** Wild-type cells expressing recombinant HV-*Lm*DAT fusion were analyzed by DIC (*panel 1*) or immunofluorescence microscopy using anti-V5 monoclonal antibody (*panel 2*) or hypoxanthine-guanine phosphoribosyltransferase polyclonal antibodies (*panel 3*). *Panel 4*, merge of *panels 2* and *3*. *Panels 5* and *6*, DIC (*panel 5*) and immunofluorescence analysis using anti-V5 antibody (*panel 6*) in wild-type non-transfected control cells.

on complete media containing either glucose or galactose as a sole carbon source. As expected, both strains grew on galactose-containing media, which promotes expression of the *GAT1* transgene (Fig. 4*A*). However, whereas the *gat1*Δ*gat2*Δ+[*GAL1*::*GAT1*]+[*ADH1*::*LmDAT*] strain was capable of growing on glucose-containing media that represses *GAT1* expression, the *gat1*Δ*gat2*Δ+[*GAL1*::*GAT1*] +[*ADH1*] failed to give colonies on this medium, suggesting that *LmDAT* complements the loss of the endogenous *GAT1* and *GAT2* genes. We next selected 5-fluoroorotate-resistant derivatives of the *gat1*Δ*gat2*Δ+[*GAL1*::*GAT1*]+[*ADH1*::*LmDAT*] strain that lost *pGAL1*::*GAT1 URA3* plasmid. Consequently, a strain *gat1*Δ*gat2*Δ+[*ADH1*::*LmDAT*], which lacks yeast *GAT1* and *GAT2* genes and relies for survival solely on *LmDAT*, was successfully obtained, thus eliminating the

possibility of complementation due to expression of the endogenous *GAT1* gene. The presence of *LmDAT* or the absence of the episome expressing the *GAT1* gene in this strain was verified by PCR analyses using primers specific to *GAT1* and *LmDAT* (Fig. 4*B*). As a positive control, PCR analyses using primers specific for the choline transporter gene *HNM1* showed the presence of this gene in all strains (Fig. 4*B*). Together, these data demonstrate that *Lm*DAT can functionally complement the loss of the yeast dual DHAPAT/GPAT acyltransferase activity.

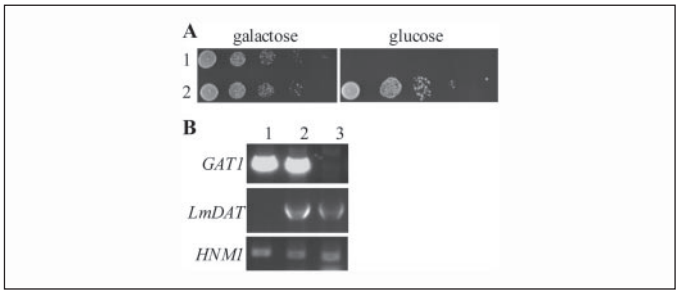

FIGURE 4. ***LmDAT* complements the lethal phenotype of a yeast double mutant lacking GPAT and DHAPAT activity.** *A*, growth assay of *gat1*Δ*gat2*Δ+[*GAL1*::*GAT1*]+[*ADH1*] (*1*) and *gat1*Δ*gat2*Δ+[*GAL1*::*GAT1*]+[*ADH1*::*LmDAT*] (*2*) serially 10-fold diluted on complete medium containing either glucose or galactose as sole carbon source. The highest dilution contains 3×10^4 cells. Plates were incubated at 30 °C for 4 days. *B*, agarose gel electrophoresis of PCR products obtained by amplifying genomic DNA from *gat1*Δ*gat2*Δ+[*GAL1*::*GAT1*] (*1*), *gat1*Δ*gat2*Δ+[*GAL1*::*GAT1*]+[*ADH1*::*LmDAT*], (*2*), and *gat1*Δ*gat2*Δ+[*ADH1*::*LmDAT*](3) with *GAT1*-, *LmDAT*-, and *HNM1*-specific (positive control) primers as described under "Experimental Procedures."

We next characterized the activity of recombinant *Lm*DAT in yeast. *Lm*DAT DHAPAT activity measured in the complemented cell extracts at 30 °C was linear for ~6 min before reaching a plateau. In contrast, only minimal activity could be detected when the assay was carried out at 0 °C (Fig. 5*A*). The DHAP concentration in the reaction mixture was varied to obtain a substrate saturation curve. DHAPAT activity was optimal at a substrate concentration of ~2 mM, and from the Michaelis-Menten representation, a K_m of 0.69 ± 0.06 mM and a V_{max} of 2.39 ± 0.36 nmol/min × mg were obtained (Fig. 5*B*). The specificity of the fatty acyl-CoA donor was then determined by testing different chain lengths and saturated/non-saturated fatty acyl-CoA donors. *Lm*DAT showed the best activity with palmitoyl-CoA. Lower activity was obtained with lauroyl-, myristoyl-, palmitoleoyl-, stearoyl-, linoleoyl-, oleoyl-, and arachidoyl-CoA (Fig. 5*C*). These results are consistent with the fatty acid composition of *Leishmania* membranes where C16, C18 fatty acids prevail (3, 28) and with the activity of the endogenous enzyme. To assess whether *Lm*DAT can also acylate G3P, GPAT assays were performed. Although GPAT activity could be detected in *Lm*DAT-expressing cells, this activity represented only ~8.5% of its DHAPAT activity (Fig. 5*D*).

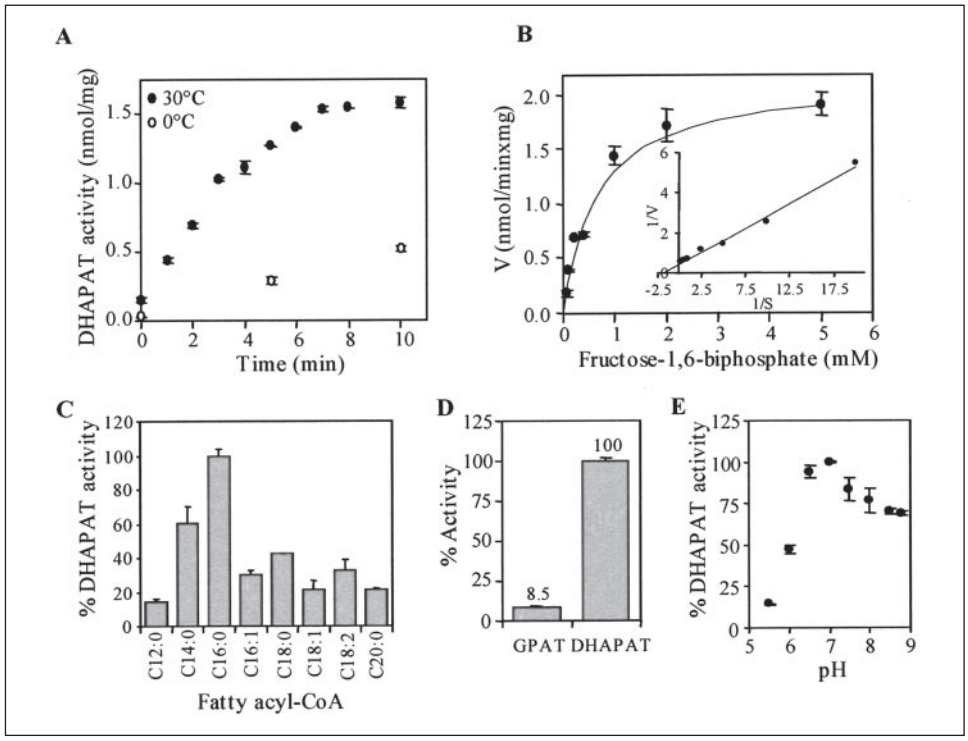

FIGURE 5. **GPAT and DHAPAT activities of *Lm*DAT expressed in *S. cerevisiae*.** The acylation rate of DHAP produced by catabolism of fructose 1,6-bisphosphate by an aldolase and triose phosphate isomerase measured as described under "Experimental Procedures." *A*, time-dependent DHAPAT activity from cell extracts of *gat1*Δ*gat2*Δ+[*ADH1*::*LmDAT*] grown in YPD. The assay was performed as described under "Experimental Procedures." *B*, kinetics of DHAPAT activity of *Lm*DAT. The substrate saturation curve was fitted to the Michaelis-Menten equation, and the double reciprocal plot is depicted as an inset. K_m and V_{max} were calculated to be 0.69 ± 0.06 mM and 2.39 ± 0.36 nmol/min × mg. *C*, fatty acyl-CoA donor specificity of *Lm*DAT. Samples were incubated at 30 °C for 5 min in the presence of 100 mM fatty acyl-CoA. *D*, DHAPAT activity of *Lm*DAT represents only 8.5±% of GPAT activity. GPAT activity of *Lm*DAT performed in the presence of 100 mM palmitoyl-CoA during 5 min. *E*, *Lm*DAT activity is pH-dependent. All assays were performed at least twice, and only one representative experiment is depicted. The S.D. is shown.

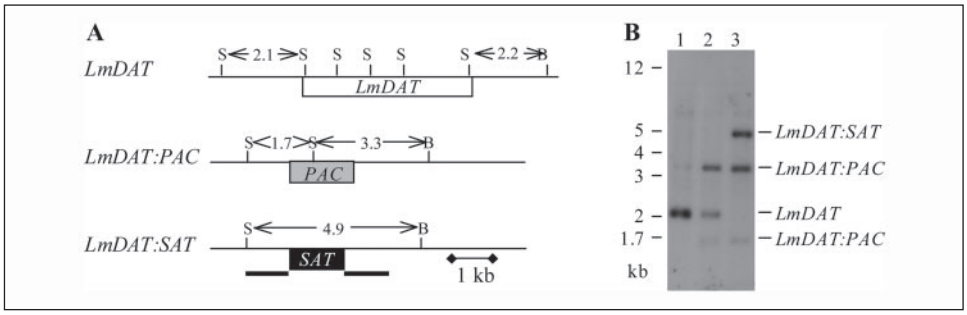

FIGURE 6. **Generation of an *LmDAT* null mutant of *L. major*.** *A*, genomic organization of the *LmDAT* locus in the wild-type and mutant versions of the allele. The probe (*thick black line*) and scale are depicted. *B*, Southern blot analysis of genomic DNA digested with BamHI and SalI. *Lane 1*, wild type; *lane 2*, the heterozygote mutant (*LmDAT*:*PAC*/*LmDAT*) with *PAC*-replaced allele; *lane 3*, homozygote mutant (*LmDAT*:*PAC*/*LmDAT*:*SAT*) with both *LmDAT* alleles replaced with *PAC* and *SAT* cassettes, respectively. The size and identity of the bands are shown. The probe used is depicted in *A*.

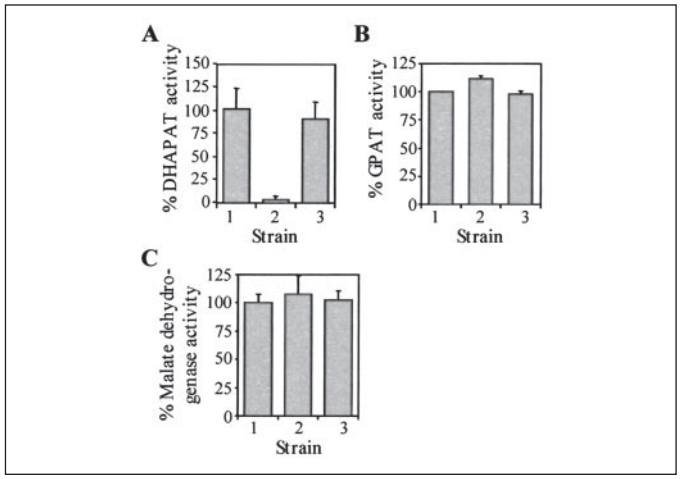

FIGURE 7. **Δ*lmdat*/Δ*lmdat* null mutant lacks DHAPAT activity.** DHAPAT (*A*), GPAT (*B*), and malate dehydrogenase (*C*) activities of wild type (*1*), null mutant Δ*lmdat*/Δ*lmdat* (*2*), and complemented (*3*) strains were assayed as described under "Experimental Procedures." For DHAPAT and GPAT assays, samples were incubated at 30 °C for 5 min in the presence of 100 μM palmitoyl-CoA. The three assays were carried out twice in duplicate, and one representative experiment is depicted. S.D. are shown.

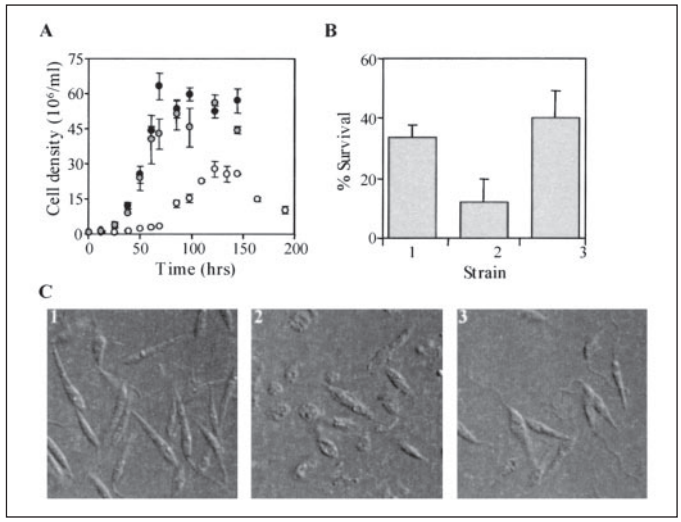

FIGURE 8. **Growth defects of the Δ*lmdat*/Δ*lmdat* mutant.** *A*, growth assay. Wild type (*black circles*), Δ*lmdat*/Δ*lmdat* (*open circles*), and Δ*lmdat*/Δ*lmdat*+[*LmDAT BSD*] (*gray circles*) were seeded at 5×10^5/ml and enumerated as a function of time with a hemacytometer. *B*, limiting dilution assays. Wild type (*1*), Δ*lmdat*/Δ*lmdat* (*2*), and Δ*lmdat*/Δ*lmdat*+[*LmDAT BSD*] (*3*) strains were diluted to 5 parasites/ml 3 days after they reached maximum cell density and transferred into 96-well plates, and parasite growth was monitored 2 weeks later. The number of parasite-containing wells is represented in percentages. These assays were performed at least twice in duplicate, and a representative experiment with S.D. is represented. *C*, DIC images were taken from cells 3 days after they reached their maximum cell density.

*Lm*DAT DHAPAT activity was optimal at a neutral pH, decreased by 30% at pH 9, and was almost absent at pH 5.5 (Fig. 5*E*).

L. major Lacking LmDAT Gene Are Deficient in DHAPAT Activity—To assess the role of *Lm*DAT in parasite physiology, a null mutant was generated. Two rounds of transformation and selection were performed to obtain the homozygous knock-out mutant. The first and second alleles were replaced by a puromycin (*PAC*) and a nourseothricin (*SAT*) cassette, respectively. A line, Δ*lmdat*/Δ*lmdat*, carrying both mutations was obtained, and the loss of the endogenous *LmDAT* alleles was verified by Southern blot analysis (Fig. 6). This result demonstrates that *LmDAT* is not essential for parasite viability. The DHAPAT activity of the Δ*lmdat*/Δ*lmdat* null mutant was compared with its isogenic parental strain (wild type) and to a Δ*lmdat*/Δ*lmdat*+[*LmDAT BSD*] complemented strain, carrying a wild-type *LmDAT* gene on an episome in the Δ*lmdat*/Δ*lmdat* knock-out background. Although the wild-type and complemented lines exhibited comparable DHAPAT activity levels, the mutant completely failed to acylate DHAP (Fig. 7*A*). This result suggests that *Lm*DAT is the sole DHAPAT enzyme in *L. major* promastigotes. To assess whether the loss of DHAPAT activity in the Δ*lmdat*/Δ*lmdat* mutant could be compensated by an increase in the cellular GPAT activity catalyzed by the *Lm*GAT enzyme, GPAT activity of the Δ*lmdat*/Δ*lmdat* was compared with that of the wild-type and complemented strains. No differences in GPAT activity could be detected between the three strains (Fig. 7*B*). As a control, similar levels of the malate dehydrogenase activity that is not related to lipid metabolism were found in the three strains (Fig. 7*C*).

L. major Lacking LmDAT Gene Have Altered Growth during Exponential Phase and Increased Cell Death during Stationary Phase—Growth assays revealed that the null mutant Δ*lmdat*/Δ*lmdat*, although viable, grew at a ~45–50% reduced growth rate when compared with wild-type cells (Fig. 8*A*; Table 2). This growth defect could be compensated by the addition of the *Lm*DAT gene. The doubling time of biomass accumulation was 14.2 ± 2.5 h for Δ*lmdat*/Δ*lmdat* mutant cells *versus* 7.6 ± 0.5 h for wild-type and 7.9 ± 0.7 h for complemented cells (Fig. 8*A*; Table 2). Furthermore, the Δ*lmdat*/Δ*lmdat* mutant reached only half the maximal cell density compared with that of the wild type and the complemented strains (~3×10^7 *versus* ~6×10^7 cells/ml; Fig. 8*A*). These results demonstrate that *LmDAT* plays an important role in parasite development during the linear phase of cellular division. Interestingly, whereas the cell number of wild-type and complemented strains remained the same several days after they reached their maximum cellular density, the cell number of the Δ*lmdat*/Δ*lmdat* mutant dramatically decreased soon after reaching its maximum cellular density (Fig. 8*A*). Microscopic analysis revealed a major alteration in the morphology of the Δ*lmdat*/Δ*lmdat* cells with an increase in the number of unflagellated, rounded, and lysed cells in the culture (Fig. 8*C*). This defect was not observed during the linear phase of growth of the Δ*lmdat*/Δ*lmdat* mutant (data not shown). In contrast, the morphology of wild-type and complemented cells was unaltered during exponential and stationary phases of growth (Fig. 8*C*).

TABLE 2
***Leishmania* doubling time (*T*) in hours**

Strains	*T*
Wild type	7.6 ± 0.5
Δ*lmdat*/Δ*lmdat*	14.2 ± 2.5
Δ*lmdat*/Δ*lmdat* [*LmDAT BSD*]	7.9 ± 0.7

We further analyzed cell survival during the stationary phase by plating wild type, knock-out, and complemented strains on fresh media and counting the number of resulting colonies. The null mutant Δ*lmdat*/Δ*lmdat* gave ~70% decreased colony number when compared with wild-type and complemented cells (Fig. 8*B*). These results demonstrate that *LmDAT* is essential for cell viability during the stationary phase. Parasite death after maximum growth was further demonstrated using PrI to stain necrotic cells followed by quantification of PrI-positive cells by flow cytometry. Wild-type, knock-out, and complemented cells did not take up PrI during the logarithmic phase of development and replication (Fig. 9*A*). Upon entry into stationary phase, however, 14% of Δ*lmdat*/Δ*lmdat* cells were permeable to this dye, whereas only ~1–2% of wild-type and complemented cells were PrI-positive (Fig. 9*B*).

L. major Lacking LmDAT Gene Are Avirulent—To examine the role of *LmDAT* in *L. major* virulence, wild-type, null mutant, and complemented strains were examined for their ability to form a footpad lesion using a mouse model of cutaneous leishmaniasis. Whereas wild-type

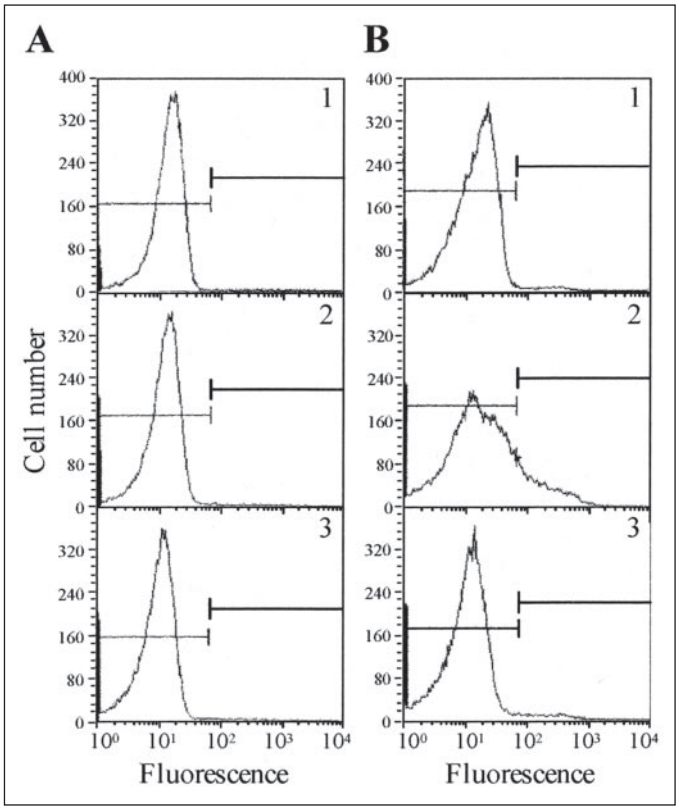

FIGURE 9. **Flow cytometry of PrI stained *Leishmania* parasites.** End-log phase (*A*) or 3-day stationary phase (*B*) promastigotes were incubated in the presence of PrI as described under "Experimental Procedures." Then ~5,000 cells were analyzed by flow cytometry. *1*, wild type; *2*, Δ*lmdat/*Δ*lmdat*; 3, Δ*lmdat/*Δ*lmdat*+[*LmDAT BSD*].

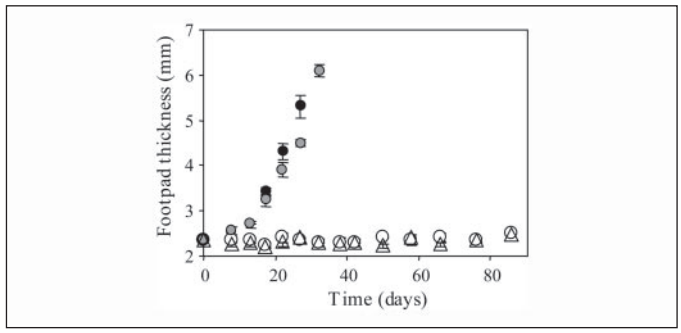

FIGURE 10. **The Δ*lmdat/*Δ*lmdat* mutant is avirulent.** Groups of four mice were injected with 10^6 wild type (*black circles*), 10^6 complemented line Δ*lmdat/*Δ*lmdat*+[*LmDAT BSD*] (*gray circles*) or either 10^6 (*open circles*) or 10^7 (*open triangles*) Δ*lmdat/*Δ*lmdat* mutant parasites as described under "Experimental Procedures," and lesion formation was followed. The thickness of the footpad was measured with a vernier caliper.

and complemented strains formed a lesion within 4 weeks after injection with 10^6 parasites, no lesions could be detected in mice injected with the null mutant 11 weeks post-injection with 10^6 or 10^7 parasites (Fig. 10).

DISCUSSION

The characterization of the enzymatic machinery involved in the initiation of glycerolipid biosynthesis in *Leishmania* is essential for understanding how the parasite synthesizes its virulence factors and develops and multiplies to cause the pathological symptoms associated with human leishmaniasis. Two reactions initiate the glycerolipid biosynthetic pathway, acylation of G3P by a GPAT enzyme or of DHAP by a DHAPAT. We have previously shown that in *Leishmania*, the GPAT enzyme *Lm*GAT is not essential for promastigote development and survival and that mutants lacking this gene were affected in the synthesis of triglycerides but had unaltered synthesis of the major ester and ether phospholipids and were as virulent as wild-type cells in a mouse model of cutaneous leishmaniasis (27). To understand the importance of the alternative pathway (acylation of DHAP) in parasite physiology, we have isolated the gene *LmDAT* encoding the DHAPAT protein, characterized its enzymatic properties, and generated a null mutant.

*Lm*DAT and its orthologs from *T. brucei* and *T. cruzi* are unusually large enzymes harboring, in addition to their C-terminal DHAPAT domain, a large N-terminal domain of 650 amino acid residues. This domain does not share homology with any known proteins in the available databases. The presence of an unusual polypeptide extension has also been found in the subunit II of RNA polymerase I of *T. brucei* and *L. major*, which harbor an N-terminal 250 amino acid extension (40, 41), and the 3-mercaptopyruvate sulfur-transferase enzymes of *L. major* and *Leishmania mexicana*, which contain 70 additional amino acids at their C terminus (42). So far no function could be assigned to these domains.

Our results showed that *LmDAT* complements the lethal phenotype of the yeast double mutant *gat1*Δ*gat2*Δ. Although yeast cells lack ether phospholipids, their GAT1 and GAT2 enzymes are capable of acylating both G3P and DHAP (32, 39). The 1-acyl-DHAP formed from DHAP is reduced by an NADPH-dependent reductase to 1-acyl-G3P, which is subsequently used for the synthesis of ester phospholipids (43, 44). Because of the strong DHAPAT activity of *Lm*DAT, its complementation of the *gat1*Δ*gat2*Δ mutant could most likely occur through the synthesis of 1-acyl-DHAP. However, we cannot exclude that the minor GPAT activity of *Lm*DAT might also contribute to this complementation. Biochemical analysis revealed that similar to mammalian DHAPATs, *Lm*DAT exhibits a low affinity for DHAP with a K_m of ~0.7 mM and shows the best activity in the presence of palmitoyl-CoA (15, 18, 45, 46). The latter result contrasts with *Lm*GAT, that was more promiscuous in term of fatty acyl-CoA donor, preferring longer unsaturated fatty-acyl-CoAs (27).

Our studies provide several lines of evidence supporting the idea that *Lm*DAT is a single DHAPAT enzyme in *L. major*. First, the biochemical properties of recombinant *Lm*DAT are identical to those measured from *Leishmania* promastigote extracts. Second, the null mutant Δ*lmdat/*Δ*lmdat* lacking *LmDAT* gene is deficient in DHAPAT activity. Third, low stringency hybridization analyses revealed that *LmDAT* is a single copy gene in the *L. major* genome (data not shown). Fourth, no other DHAPAT homologs could be identified in the available *L. major* sequence data base.

Mammalian cells harbor one GPAT in the endoplasmic reticulum, two in the mitochondria, and a DHAPAT in peroxisomes, whereas plants lack DHAPAT but have a battery of GPAT isoforms localized in different subcellular compartments such as chloroplast, cytoplasmic membranes, and mitochondria and expressed in a tissue-specific manner (Refs. 47 and 48; for review, see Refs. 49–51). On the other hand, yeast expresses two unique enzymes, GAT1 and GAT2, that acylate both G3P and DHAP with similar efficiency (32, 39). Interestingly, *Leishmania* represents an unusual situation, harboring a single GPAT enzyme encoded by *LmGAT* and a single DHAPAT, encoded by *Lm*DAT (Ref. 27 and this work).

Previous studies showed that deletion of the *LmADS* gene of *L. major*, which encodes an alkyl dihydroxyacetone phosphate synthase (ADS), results in severe alteration in the synthesis of ether lipids but had no effect on the synthesis of ester phospholipids or promastigote growth (28). Furthermore, we demonstrated that a Δ*lmgat/*Δ*lmgat* mutant lacking GPAT activity, while affected in the synthesis of triglycerides, was unaltered in the

synthesis of ester phospholipids and showed normal growth in logarithmic and stationary phases (27). Thus, the slow growth phenotype of the Δ*lmdat*/Δ*lmdat* mutant and its accelerated death in stationary phase are unlikely to be due to loss of synthesis of ether lipids or reduced synthesis of triglycerides. Therefore, we propose that the acylation of DHAP by *Lm*DAT may represent the primary route for the synthesis of ester phospholipids in this parasite and that abrogation of this metabolic pathway is responsible for the slow growth phenotype. Alternatively, because glycolysis in *Leishmania* and related protozoa occurs within the glycosomes (52), it is possible that deletion of *Lm*DAT may lead to increased levels of DHAP within these organelles. Accumulation of this precursor has previously been shown to be deleterious to *Leishmania* (53). Studies to evaluate these two hypotheses are warranted.

The slow growth phenotype and accelerated death after entry into the stationary cell stage of the Δ*lmdat*/Δ*lmdat* strain are reminiscent of a *Leishmania* mutant devoid of sphingolipids (54). Similar to fungi, *Leishmania* contains mainly inositol phosphoceramide instead of sphingomyelin or glycosphingolipid in its membranes. Deletion of *LmDAT* may impair inositol phosphoceramide biosynthesis indirectly because of a lack of the precursor phosphatidylinositol.

A significant finding reported in this paper is the attenuated virulence phenotype of *L. major* resulting from the deficiency of *LmDAT*. Although the exact mechanism by which *Lm*DAT promotes virulence remains to be elucidated, the Δ*lmdat*/Δ*lmdat* mutant might be considered as a vaccine candidate.

The phenotype of the Δ*lmdat*/Δ*lmdat* mutant is more severe than that of the Δ*ads*/Δ*ads* mutant, which lacks ether lipids, or that of the Δ*lpg1*/Δ*lpg1* mutant, which lacks lipophosphoglycan (28, 55). This difference is not surprising because *LmDAT*-deficient parasites die rapidly upon entry into the stationary cell stage. Cessation of growth at high cell density has been shown to trigger differentiation to metacyclics (56). Thus, very likely the Δ*lmdat*/Δ*lmdat* mutant does not differentiate into the virulent metacyclic form of the parasite, which is pre-adapted for survival in the vertebrate host. Also, because *L. major* harbors ether-lipid-based virulence factors such as lipophosphoglycan and glycosylphosphatidylinositol-anchored proteins, we surmise that their biosynthesis might be affected in this strain and, thus, contribute to the attenuation of virulence.

Acknowledgments—We thank A. Jardim for the generous gift of hypoxanthine-guanine phosphoribosyltransferase antiserum. S. M. Beverley is greatly appreciated for the plasmids pXG.SAT and pX63.PAC. We thank Dr. Asis Das, University of Connecticut Health Center and the anonymous reviewers for constructive comments on the manuscript.

REFERENCES

1. Wassef, M. K., Fioretti, T. B., and Dwyer, D. M. (1985) *Lipids* **20,** 108–115
2. Beach, D. H., Holz, G. G., Jr., and Anekwe, G. E. (1979) *J. Parasitol.* **65,** 201–216
3. Chaudhuri, G., and Banerjee, A. B. (1987) *Indian J. Med. Res.* **85,** 140–148
4. Descoteaux, A., and Turco, S. J. (2002) *Microbes Infect.* **4,** 975–981
5. Ilg, T. (2001) *Med. Microbiol. Immunol.* **190,** 13–17
6. Matlashewski, G. (2001) *Med. Microbiol. Immunol.* **190,** 37–42
7. Naderer, T., Vince, J. E., and McConville, M. J. (2004) *Curr. Mol. Med.* **4,** 649–665
8. Sacks, D. L. (2001) *Cell. Microbiol.* **3,** 189–196
9. Croft, S. L., Seifert, K., and Duchene, M. (2003) *Mol. Biochem. Parasitol.* **126,** 165–172
10. Soto, J., Arana, B. A., Toledo, J., Rizzo, N., Vega, J. C., Diaz, A., Luz, M., Gutierrez, P., Arboleda, M., Berman, J. D., Junge, K., Engel, J., and Sindermann, H. (2004) *Clin. Infect. Dis.* **38,** 1266–1272
11. Jha, T. K., Sundar, S., Thakur, C. P., Bachmann, P., Karbwang, J., Fischer, C., Voss, A., and Berman, J. (1999) *N. Engl. J. Med.* **341,** 1795–1800
12. Sundar, S., Rosenkaimer, F., Makharia, M. K., Goyal, A. K., Mandal, A. K., Voss, A., Hilgard, P., and Murray, H. W. (1998) *Lancet* **352,** 1821–1823
13. Hajra, A. K., and Bishop, J. E. (1982) *Ann. N. Y. Acad. Sci.* **386,** 170–182
14. de Vet, E. C., Hilkes, Y. H., Fraaije, M. W., and van den Bosch, H. (2000) *J. Biol. Chem.* **275,** 6276–6283
15. Hajra, A. K. (1995) *Prog. Lipid Res.* **34,** 343–364
16. Liu, D., Nagan, N., Just, W. W., Rodemer, C., Thai, T. P., and Zoeller, R. A. (2005) *J. Lipid Res.* **46,** 727–735
17. Jones, C. L., and Hajra, A. K. (1983) *Arch. Biochem. Biophys.* **226,** 155–165
18. Ofman, R., and Wanders, R. J. (1994) *Biochim. Biophys. Acta* **1206,** 27–34
19. Webber, K. O., and Hajra, A. K. (1993) *Arch. Biochem. Biophys.* **300,** 88–97
20. LaBelle, E. F., Jr., and Hajra, A. K. (1972) *J. Biol. Chem.* **247,** 5825–5834
21. Heise, N., and Opperdoes, F. R. (1997) *Mol. Biochem. Parasitol.* **89,** 61–72
22. Biermann, J., Just, W. W., Wanders, R. J., and Van Den Bosch, H. (1999) *Eur. J. Biochem.* **261,** 492–499
23. Thai, T. P., Heid, H., Rackwitz, H. R., Hunziker, A., Gorgas, K., and Just, W. W. (1997) *FEBS Lett.* **420,** 205–211
24. Ofman, R., Hettema, E. H., Hogenhout, E. M., Caruso, U., Muijsers, A. O., and Wanders, R. J. (1998) *Hum. Mol. Genet.* **7,** 847–853
25. Barth, P. G., Wanders, R. J., Schutgens, R. B., and Staalman, C. R. (1996) *Am. J. Med. Genet.* **62,** 164–168
26. Moser, H. W. (1993) *Adv. Hum. Genet.* **21,** 1–106 and 443–151
27. Zufferey, R., and Ben Mamoun, C. (2005) *Mol. Microbiol.* **56,** 800–810B. C.
28. Zufferey, R., Allen, S., Barron, T., Sullivan, D. R., Denny, P. W., Almeida, I. C., Smith, D. F., Turco, S. J., Ferguson, M. A., and Beverley, S. M. (2003) *J. Biol. Chem.* **278,** 44708–44718
29. Ngo, H., Tschudi, C., Gull, K., and Ullu, E. (1998) *Proc. Natl. Acad. Sci. U. S. A.* **95,** 14687–14692
30. Miller, C. A., III, Martinat, M. A., and Hyman, L. E. (1998) *Nucleic Acids Res.* **26,** 3577–3583
31. Gueiros-Filho, F. J., and Beverley, S. M. (1997) *Science* **276,** 1716–1719
32. Zaremberg, V., and McMaster, C. R. (2002) *J. Biol. Chem.* **277,** 39035–39044
33. Santiago, T. C., Zufferey, R., Mehra, R. S., Coleman, R. A., and Ben Mamoun, C. (2004) *J. Biol. Chem.* **279,** 9222–9232B. C.
34. Bates, E. J., and Saggerson, E. D. (1979) *Biochem. J.* **182,** 751–762
35. Lewin, T. M., Wang, P., and Coleman, R. A. (1999) *Biochemistry* **38,** 5764–5771
36. Coleman, R. A., Lewin, T. M., and Muoio, D. M. (2000) *Annu. Rev. Nutr.* **20,** 77–103
37. Sommer, J. M., and Wang, C. C. (1994) *Annu. Rev. Microbiol.* **48,** 105–138
38. Shih, S., Hwang, H. Y., Carter, D., Stenberg, P., and Ullman, B. (1998) *J. Biol. Chem.* **273,** 1534–1541
39. Zheng, Z., and Zou, J. (2001) *J. Biol. Chem.* **276,** 41710–41716
40. Schimanski, B., Klumpp, B., Laufer, G., Marhofer, R. J., Selzer, P. M., and Gunzl, A. (2003) *Mol. Biochem. Parasitol.* **126,** 193–200
41. Dasgupta, A., Sharma, S., Das, A., Sarkar, D., and Majumder, H. (2002) *Med. Sci. Monit.* **8,** 341–350
42. Williams, R. A., Kelly, S. M., Mottram, J. C., and Coombs, G. H. (2003) *J. Biol. Chem.* **278,** 1480–1486
43. Athenstaedt, K., and Daum, G. (2000) *J. Biol. Chem.* **275,** 235–240
44. Athenstaedt, K., Weys, S., Paltauf, F., and Daum, G. (1999) *J. Bacteriol.* **181,** 1458–1463
45. Declercq, P. E., Haagsman, H. P., Van Veldhoven, P., Debeer, L. J., Van Golde, L. M., and Mannaerts, G. P. (1984) *J. Biol. Chem.* **259,** 9064–9075
46. Hajra, A. K. (1968) *J. Biol. Chem.* **243,** 3458–3465
47. Lewin, T. M., Schwerbrock, N. M., Lee, D. P., and Coleman, R. A. (2004) *J. Biol. Chem.* **279,** 13488–13495
48. Zheng, Z., Xia, Q., Dauk, M., Shen, W., Selvaraj, G., and Zou, J. (2003) *Plant Cell* **15,** 1872–1887
49. Athenstaedt, K., and Daum, G. (1999) *Eur. J. Biochem.* **266,** 1–16
50. Dircks, L., and Sul, H. S. (1999) *Prog. Lipid Res.* **38,** 461–479
51. Murata, N., and Tasaka, Y. (1997) *Biochim. Biophys. Acta* **1348,** 10–16
52. Opperdoes, F. R., and Borst, P. (1977) *FEBS Lett.* **80,** 360–364
53. Helfert, S., Estevez, A. M., Bakker, B., Michels, P., and Clayton, C. (2001) *Biochem. J.* **357,** 117–125
54. Zhang, K., Showalter, M., Revollo, J., Hsu, F. F., Turk, J., and Beverley, S. M. (2003) *EMBO J.* **22,** 6016–6026
55. Späth, G. F., Epstein, L., Leader, B., Singer, S. M., Avila, H. A., Turco, S. J., and Beverley, S. M. (2000) *Proc. Natl. Acad. Sci. U. S. A.* **97,** 9258–9263
56. Sacks, D. L., and Perkins, P. V. (1984) *Science* **223,** 1417–1419